The Dynamic Model of the Automatic Clamping Mechanism with a Rotating Input Link

Borys Prydalnyi[(✉)] [ID]

Lutsk National Technical University, 75, Lvivska St., Lutsk 43018, Ukraine
`b.prydalnyi@lutsk-ntu.com.ua`

Abstract. Some features of a new design of clamping mechanism drive for automatic fixing of cylindrical objects in metalworking machines are considered. One of the proposed design features is a rotating input link, which receives input energy in the form of rotational motion. The presented drive's operation is considered a part of the clamping mechanism with a collet chuck. Furthermore, the clamping mechanism's interaction with a drive of the main movement of a lathe is described. The dynamic model is presented as a system with lumped parameters, consisting of rigid bodies connected by inertialess elastic-dissipative links. The stages of the backlash elimination and conversion of the mechanism elements' kinetic energy into the system's stressed state's potential energy are considered separately. The obtained results can contribute to the development of methods for calculating this type's structures' parameters. They can be helpful in the determination of more optimal geometric-mass parameters of the elements of these structures.

Keywords: Clamp drive · Spindle assembly · Lathe

1 Introduction

It is known that the productivity of processing on metalworking machines can be improved by increasing the cutting modes. That is, it is necessary to increase the rate of chip removal or chip load. Increasing the spindle assembly's rotation speed (SA) requires improving the dynamic characteristics of its design and the ability to balance accurately and more [1, 2]. Increasing the feed during machining increases the cutting forces acting on the object fixed (tool or workpiece) and requires an increase in the clamping forces for effective fixation. Providing the required parameters for clamping workpiece or cylindrical tool in metalworking machines depends on the clamping mechanism (CM) operation, which is part of the SA. One of the main and largest subsystems of the CM is its drive (actuator) ACM. For eliminating these shortcomings and improving the conditions of workpiece processing, a new ACM design [3] was developed.

2 Literature Review

Several scientific papers present mathematical models and studies of spindle assemblies' characteristics as a single system without singling out clamping mechanisms.

The operation principles of new clamping mechanisms of the CNC lathe are described in [4]. Mathematical models of trajectories spindle with lumped parameters have been developed [5]. In [6], ultra-precision spindle's dynamic properties at different speeds are investigated using experimental impact tests. Machine tool dynamics is modeled using the finite element approach [7]. Using the design matrix, a flow-chart for the dynamics design method coupled with multisource information was obtained in [8]. In [9], carbon fiber reinforced plastic is described as a promising material for enhancing machine tools' spindle performance. The paper [10] covers diagnostics and monitoring CNC machine tools, industrial robots, and production lines. The paper [11] proposes an alternative method of balancing motorized spindles based on the real-time position data of CNC machine tools to reduce the costs associated with external balancing instruments and improve the dynamic balancing process's efficiency. The method of estimation the cutting forces and vibrations at the milling tool from accelerometers mounted on the spindle housing is presented in [12]. A specific electromagnetic excitation device is used to measure the Frequency Response Function of the spindle at high speeds, and the evolution with the speed of the eigenfrequencies and the radial stiffness is analyzed in [13]. In the paper [14] an experimental approach based on accurate characterizations of the dynamic behavior for different spindle conditions (repaired or damaged) is proposed. For improving the spindle system during the design and predict the tool dynamics, the paper [15] proposes modeling of spindle-holder assembly and presents an investigation on the contact characteristic under clamping and centrifugal forces. The paper [16] examines the influence of different clamping chucks on energy consumption parameters, tool wear, and surface qualities, thereby focusing on important sustainability indicators in machining operations. In [17], clamping force-deformation characteristics are plotted for implementing a corrective clamping mechanism to control workpiece deformations. In the study [18], experimental studying has been carried out for discussing dynamic characteristics of spindle imbalance, which induces forced oscillations and the impact on surface generation during diamond turning. For minimizing the duration of the clamping and unclamping processes, it is necessary to ensure the high speed of the CM and, as a result, significant acceleration of its elements. This shows the feasibility of analyzing the dynamic characteristics of the CM structures.

3   Research Methodology

The developed model (Fig. 1), which describes the CM's work with the new ACM, is a system with lumped parameters, comprising perfectly rigid bodies interconnected by inertial elastic-dissipative elements. The pliability and dissipative forces of internal friction in the material of only the most strained elements and the losses due to sliding friction in their conjugations were taken into account to simplify the dynamic model. For example, it does not take the spindle and rotor's torsional stiffness into account because they are much larger than other elements to neglect their torsional pliability.

The creation of the clamping force in CM with the presented ACM occurs with the torque's participation from the main motion drive (spindle rotation). The SA receives a rotational motion with torque M_{sh} and angular velocity ω_{sh} from the main electric motor through a set of gears that form a kinematic connection of the main drive with

Fig. 1. The dynamic model of the new ACM [3] as a part of CM of the lathe.

a total gear ratio i_{kz} and damping characteristics (dissipation) and stiffness k_{kz} and c_{kz} respectively. The main electric motor drive's stator interacts with the rotor with a mass m_{p1} through an electromagnetic field with a damping factor k_{ed1} and stiffness c_{ed1}, which ensures its rotation with torque M_{d1} and angular velocity ω_{d1}. Thus, the rotor's rotation angle of the main motor drive ϕ_{d1} and the spindle ϕ_{sh} are related by the dependence $\phi_{sh} = \phi_{d1}, i_{kz} \pm \theta_{kz}$ and $\phi_d = \phi_{sh} + \phi$.

At the rear end of the spindle with mass m_{sh} (Fig. 1) there is a threaded surface with a diameter d_1 and pitch h on which the rotor of the motor ACM with the outer diameter d_2, mass m_p and moment of inertia J_p is screwed. The threaded surfaces of the spindle and rotor form a self-braking screw-type gear with a transmission ratio i_{gn}. The ACM rotor interacts with the stator through an electromagnetic field with damping k_{ed} and stiffness c_{ed} characteristics, which allows the ACM rotor to rotate to the machine body with torque M_d and angular velocity ω_d that differs from ω_{sh}. The forces of friction in the screw self-braking gear determine its damping characteristics k_{gn} and create the braking torque M_g^T. The resultant of torques M_{sh} and M_d cause the rotor's rotation relative to the spindle with force F_{a1} speed $\omega_\Delta = \omega_d - \omega_{sh}$, and axial movement of the rotor ACM approximately equal to the movement value x_T' of the output link-rod to transmit force to the clamping chuck (Fig. 1). The moments of inertia of rotation of the elements rotating together with the spindle relative to its axis are reduced to the flywheel with the moment of inertia J_{shu}^n.

The transmission of axial force F_{a1} to the clamping chuck occurs after backlash elimination $\Delta_{\Pi p}$ appears in the CM as a specific feature of the installation, adjustment, and wear. This reduces the magnitude of the axial movement of the input link of the clamping chuck by the value $x_m = x_m' - \Delta_{np}$. The axial force F_{a1} is transmitted through a set of transmission links with total stiffness $c_{\Pi p}$ and damping k_{np} to the output link-rod, collet chuck and workpiece with masses m_T, m_c and m_π respectively. The movement of these masses in the axial direction is counteracted by friction forces S_T^T, which occur mainly in the contacts of the surfaces of the spindle and the link-rod. This interaction is characterized by the damping coefficient K_T.

The processes that take place in the clamping chuck (in Fig. 1. the area is indicated by a dashed line) are presented in a simplified form. Axial movement x_T is transmitted with force F_{a1} from the link-rod to the clamping elements of the collet chuck through the petals with the coefficient of tensile deformation $c_{\Pi c}$ (Fig. 1). This causes the force

interaction in the wedge mechanism of the collet with the gear ratio i_u. The clamping elements of the collet with the mass m_{ze} is also moving in the radial direction by the value, which is counteracted by the force of elastic deformation of the collet petals with a coefficient $c_{\Pi c}^\gamma$. When the clamping elements are moving in the radial direction, it causes the backlash elimination (mainly between the surfaces of the workpiece and the clamping elements) with the total value Δ_k, and the workpiece is clamping with effort $F_{\gamma 2}$. The contact characteristics of the clamping elements with the spindle and the workpiece and the size of the gaps are described by the coefficient of elasticity c_k, damping K_k, and the size of the gap $\Delta_K = (d_c - d_\Pi)$, where d_c, d_Π are the diameters of the collet hole and the workpiece, respectively.

The rotation of the ACM rotor in the opposite direction to the spindle rotation can be obtained when the ACM engine is running in the mode of electric machine brake. One of the recommended modes is regenerative braking, which provides certainty of the rotor speed ω_d, which it seeks to achieve due to braking – synchronous motor frequency. This improves the conditions for regulation the work of ACM – obtaining the required value ω_Δ. The maximum torque M_d on the rotor ACM in this mode is slightly higher than in the driving mode due to resistance losses in the stator, which in the driving mode leads to a decrease in torque, and in the generator – to additional use (consumption) of the external driving torque, ie. braking.

Two variants of the initial operating conditions of the ACM can be distinguished at $\omega_d = \omega_{sh}, (\omega_\Delta = 0)$: SA is stopped $\omega_{sh} = 0$; the SA rotates $\omega_{sh} \neq 0$. When at the initial stage SA rotates ($\omega_\Delta = 0$, $\omega_{sh} \neq 0$), there are two ways to ensure the difference ω_Δ in angular velocities of the rotor and spindle ($\omega_d \neq \omega_{sh}$) for the ACM operation:

1. The ACM motor is only switched on during clamping or unclamping processes. Outside these processes, the magnetic field's influence on the rotor ACM is absent, so it rotates with the spindle under the action of the moment M_{sh} from the drive of the main motion. The process of switching on the ACM motor can be accompanied by negative effects in the CM which is associated with transients.

2. The ACM motor idles during spindle rotation and provides rotation of the rotor under the influence of torque M_π with a frequency identical to the spindle speed $\omega_d = \omega_{sh}$ ($\omega_\Delta = 0$). This requires constant monitoring of the actual speeds of the spindle and rotor ACM and their coordination. For performing clamping (unclamping), the current characteristics U, I, υ are changed by the controller device to ensure rotation of the rotor with an angular velocity ω_d that differs in modulus or direction from the angular velocity of the spindle ω_{sh} by a given value $\omega_\Delta = \omega_d - \omega_{sh}$.

Depending on the parameters of the CM's elements with ACM, control system, and method of obtaining ω_Δ. the number of stages of its work may be different. In the most general case, we can distinguish two stages of the CM:

1. Transients in ACM during its uncontrolled acceleration from the state of rest and the absence of resistance forces on the output link to the output axial force's appearance. This stage is characterized by the beginning of the movement and active acceleration of moving masses during backlash elimination $\Delta_{\Pi p}$ and Δ_K without the emergence of

deformations of links and tension in the system. Energy is also spent on overcoming friction forces. There is an increase in the kinetic energy of the CM

2. The value of the axial force on the output link increases from zero to the maximum steady-state, which is accompanied by the appearance of elastic deformations of the links of the CM (the appearance of the stress state of the system). The kinetic energy of the motion of the CM links is transformed into the potential energy of the stress state of the system. The engine ACM rotor rotation speed rapidly approaches the spindle rotation speed, which ends with self-braking in the screw-type gear.

The nature of the transients during the operation of the CM depends on the features of its design. Backlashes θ_{KZ}, $\Delta_{\Pi p}$ and Δ_K which exist in the kinematic pairs of the CM, are expressed in the form of a conditional resulting angular gap which is reduced to the input link and can determine the features of operating the CM at the initial stage. If this angular backlash's magnitude is significant, then the transient electromagnetic process associated with the ACM motor's start can be considered completed during the backlash elimination. It means that before the ACM motor starts work under the load from the resistance torque, there is the process of some free run with non-zero initial speed and torque. In the mathematical model, this can be expressed by other initial conditions and the appearance of an additional equation of motion. In the case of small gaps in the kinematic pairs, we can assume that the torque of resistance applies to the rotor ACM at the initial moment of start-up and remains invariant for some time. Self-braking transmission with a gear ratio $i_{g\pi}$ conditionally divides the elastic-deformable torsional system of the MR into two sections. In the absence of action M_d (the ACM motor is switched off), the torque of elastic deformation $M_c = f\left(\phi, c_{\Pi p}, c_{\Pi c}, c_{\Pi c}^{\gamma}, c_K\right)$ forces can unscrew the elements of the transmission of the ACM in the opposite direction to what it was during the clamping. The self-braking screw gear transmission remains locked if elastic forces' moment does not exceed the moment of friction forces M_g^T in the transmission created during the clamp. Under these conditions, after the ACM engine shutdown, its rotor performs decaying oscillations due to the action of the CM links' elastic forces (c_{zm}) and dissipative factors with damping coefficient K_{zm} (Fig. 1). If the maximum value of the torque from elastic forces exceeds the self-braking torque M_g^T, there is braking-off (release) of the system, which reduces workpiece clamping forces and reduces ACM work reliability. To unclamp the workpiece, the condition braking-off the ACM $M_d > M_g^T$ must be met. The ACM motor creates peak torque at the initial stage due to statical friction forces. Dynamic displacements caused by the elastic characteristics of the CM links (c_{zm}) (Fig. 2) can be considered as forced oscillations (torsional) of the multi-mass system near the "equilibrium" motion of the system elements with rigid links. Oscillations are caused by the action of active forces and forces of inertia.

When the rotor's rotation speed with the moment of inertia J_p is changing by the value ω_Δ, there is a dynamic torque $M_{Jp} = J_p \frac{d\omega_\Delta}{dt} = J_p \ddot{\phi}(t)$. The rotation of the rotor relative to the spindle is also associated with the movement in the axial direction of lumped masses m_p, m_T, m_c, m_π, so the action of inertia of these links must be reduced to the rotor in the form of a moment of inertia $J_p^P = f\left(m_p,\ m_T,\ m_c,\ m_\Pi,\ m_{ze},\ i_{g\Pi},\ i_c\right)$, which corresponds to the torque $M_p^P = J_p^P \frac{d\omega_\Delta}{dt} = J_p^P \ddot{\phi}(t)$. As a result of the force interaction of the rotor with the spindle through the links of the CM (Fig. 2) with elastic-dissipative
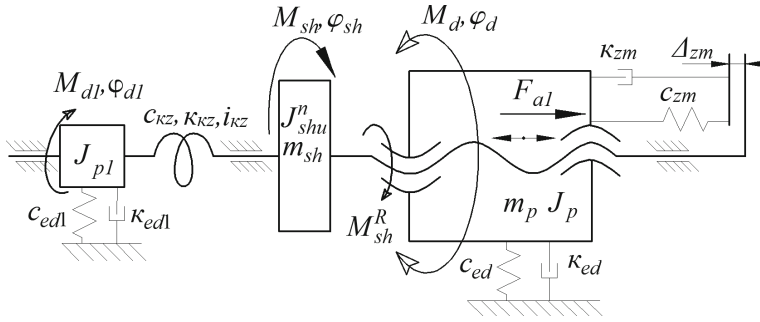
Fig. 2. Interaction of CM with other subsystems of the machine.

characteristics c_{zm} and K_{zm} there are torques from the action of elastic forces $M_c = f(\phi,\ c_{\Pi p},\ c_{\Pi c},\ c_{\Pi c}^{\gamma},\ c_k)$ and dissipative forces $M_k = f(t,\ \phi,\ K_{\pi p},\ K_T,\ K_K)$ that counteract the rotation of the rotor relative to the spindle during clamping of a workpiece. Thus, the torques M_d and M_{Jp} arising on the rotor of the ACM motor during the clamp are counterbalanced by the torque of resistance $M_R = M_K + M_C + M_{Jp}^P$ applied to the rotor from the CM.

$$M_d - M_{Jp} = M_K + M_C + M_{Jp}^P \tag{1}$$

The electromagnetic torque M_π in the mode of high deceleration $\omega_d \rightarrow \omega_{sh}$ under the action M_R can be represented as a function of speed and supply voltage $M_d = f(\dot{\phi}_d,\ U)$, and the condition of providing the required value of the clamping forces $F_{\gamma 2}$ is presented as M_d^{maxR}. If $M_d = 0$, the expression implies the condition of the clamp due to the action of inertia.

At the final stage of the clamp, the kinetic energy of motion of the CM elements is converted into the stress state's potential energy, so when the rotor slows down under the action of active forces (M_K and M_C) the value $\frac{d\omega_\Delta}{dt}$ became negative and torques M_{Jp} and M_{Jp}^P change direction. Overcoming the torque M_R of resistance of the rotor rotation relative to the spindle due to the action on the rotor of the torques M_π and M_{Jp} causes the appearance of equal in modulus and opposite in direction reactive torque $M_w^R = M_\partial - M_{Jp}$ on the spindle.

The torque M_{d1} from the main drive motor is transmitted to the SA through the gears with the common gear ratio i_{kz} and characteristics of damping K_{Kz} and stiffness c_{kz}. In the steady-state mode of rotation of the spindle at a constant speed, $\omega_{sh} = \omega_{d1} \cdot i_{kz}$ it is counteracted by the torque M_{sh} that arises as a result of the action of dissipative factors, so it fulfilled equality $M_{d1} \cdot i_{kz} = M_{sh}$. The influence of the torque M_{sh}^R that occurs during the ACM operation causes a change in the speed of rotation of the SA and causes the appearance of a dynamic torque $M_{Jsh}^P = J_{shu}^\pi \frac{d\omega_{sh}}{dt}$, which also counteracts M_{d1}. Thus the mathematical equality is fulfilled.

$$M_{d1} \cdot i_{kz} = M_{sh} + M_{sh}^R + M_{Jsh}^P \tag{2}$$

The dynamic qualities of this system, which contains the drive of the main motion and the CM with the new ACM, can be approximately estimated by the transients' duration. During the transition process, the torques M_{sh} and M_{sh}^R are constant values, the time dt corresponding to the change of the angular velocity $d\omega_{sh}$ can be determined from the equation of motion by the formula.

$$dt = J_{shu}^n \frac{d\omega_{sh}}{M_{d1} \cdot i_{kz} - M_{sh} - M_{sh}^R} \tag{3}$$

The transient processes that appear in the spindle drive resulting from operation ACM cause the change of spindle rotation speed from ω_{sh} to $\omega_{sh} + \omega_{sh}^R$. They can be found by integrating the previous expression.

$$t = \int_{\omega_{sh}}^{\omega_{sh}+\omega_{sh}^R} \frac{J_{shu}^\pi \cdot d\omega_{sh}}{M_{d1} \cdot i_{kz} - M_{sh} - M_{sh}^R} = \frac{J_{shu}^\pi \cdot \omega_{sh}^R}{M_{d1} \cdot i_{kz} - M_{sh} - M_{sh}^R} \tag{4}$$

This system's tendency to oscillations, and, as a consequence, the margin of stability can be characterized by the maximum value of the torque on the spindle $(M_{sh} + M_{sh}^R)$ relative to the steady-state value M_{sh} after the transition process.

$$G = \frac{(M_{sh} + M_{sh}^R) - M_{sh}}{M_{sh}} = \frac{M_{sh}^R}{M_{sh}} \tag{5}$$

4   Results

The mathematical description of the processes occurring during the work the CM with the new ACM and their influence on the main motion drive of the machine can be reduced to a system of equations with a description of the motion of two sections of the system – the main electromotor with transmission and the SA which are connected by elastic-deformable connection with the characteristics K_{kz}, c_{KZ} and i_{KZ} (Fig. 1, 2). The torque of the engine of the drive of the main movement $M_{\pi 1}$ is counteracted by the moments of active forces M_C^{KZ}, M_K^{KZ} and $M_{Jp1} = J_{p1} \frac{d\omega d_1}{dt} = J_{p1} \ddot{\phi}_{dt}(t)$ forces of inertia. Thus, the torque M_C^{KZ} is counteracted by the torques M_{sh} and M_{sh}^R the dynamic torque $M_{jsh}^P = J_{shu}^n \frac{d\omega_{sh}}{dt} = J_{shu}^n \ddot{\phi}_{sh}(t)$.

Therefore, the change in the rotation speeds ω_{d1} of the main drive and ACM elements depends on the magnitude of the driving moments M_{d1} and M_d. The control of the CM's characteristics with the new ACM can be performed by adjusting the values M_d and ω_d, which also affects ω_{d1} due to changes in the load on the motor of the main motion drive. The magnitude of the change ω_{d1} depends on the stiffness of the mechanical characteristics of the motor of the main motion drive, which reflects the nature of the

change in the angular velocity of the engine $\Delta\omega_{d1}$ with a change in torque ΔM_{d1}, $\beta = \frac{\Delta M_{d1}}{\Delta\omega_{d1}}$. Therefore $\omega_{d1} = f(M_d, \beta)$.

$$
\begin{cases}
M_{d1} - M_C^{kz} - M_K^{kz} = J_{p1}\dfrac{d\omega_{d1}}{dt} = J_{p1}\ddot{\phi}_{d1}(t); \\[2mm]
M_C^{kz} - M_{sh} - M_{sh}^R = J_{shu}^n \dfrac{d\omega_{sh}}{dt} = J_{shu}^n \ddot{\phi}_{sh}(t); \\[2mm]
M_C^{kz} = c_{kz}(\phi_{sh} - \phi_{d1} \cdot i_{kz} \pm \theta_{kz}); M_K^{kz} = K_{kz}\dfrac{d\phi_{dt}}{dt}; \\[2mm]
\omega_{d1} = \dfrac{\omega_{sh}}{i_{kz}}; \phi_{sh} = \phi_{d1} \cdot i_{kz}; \omega_\Delta = \omega_d - \omega_{sh}; \\[2mm]
M_{sh} = \dfrac{M_{d1}}{i_{kz}}; M_{sh}^R = M_d - M_{Jp} = M_K + M_C + M_{Jp}^P; \\[2mm]
M_C = f\left(\phi, c_{np}, c_{nc}, c_{nc}^r, c_k\right); M_K f\left(t, \dot{\phi}, k_{np}, K_T, K_k\right); \\[2mm]
M_d = f(\phi_d, U); \phi_d = \phi_{sh} + \phi; \\[2mm]
M_{Jp} = J_p \dfrac{d\omega_\Delta}{dt} = J_p \ddot{\phi}(t); M_{Jp}^P = J_p^P \dfrac{d\omega_\Delta}{dt} = J_p^P \ddot{\phi}(t).
\end{cases}
\tag{6}
$$

After substituting the second equation of the system for the first one we obtain

$$
M_{d1} - \left(J_{shu}^n \frac{d\omega_{sh}}{dt} + \frac{M_{d1}}{i_{kz}} + M_d - M_{Jp}\right) - M_K^{kz} = J_{p1}\frac{d\omega_{dt}}{dt}
$$

$$
M_{d1}\left(1 - \frac{1}{i_{kz}}\right) - K_{kz}\omega_{d1} - \dot{\omega}_{d1}\left(J_{p1} + J_{shu}^n, i_{kz} + J_p \cdot i_{kz}\right) = M_d - J_p\dot{\omega}_d \tag{7}
$$

5   Conclusions

The identified dependencies show the patterns of influence of the characteristics of themachine's main driver on the CM's operation with the new ACM. A dynamic model is compiled, and mathematical dependences are presented, which describe the geometric-mass, kinematic, and force characteristics of the CM operation. The peculiarities of the stages of the CM with the new ACM depending on the size and presence of gaps, characteristics of the elasticity of kinematic connections, the mass of elements, and specifics of control are revealed. The use of the obtained dependences promotes the development of the parametric synthesis of this type's structures.

References

1. Cisar, M., Kuric, I., Cubonova, N., Kandera, M.: Design of the clamping system for the CNC machine tool. In: 13th International Conference on Modern Technologies in Manufacturing, pp. 14–20. EDP Sciences, Cluj-Napoca (2017)
2. Mori, K., Bergmann, B., Kono, D., Denkena, B., Matsubara, A.: Energy efficiency improvement of machine tool spindle cooling system with on-off control. CIRP J. Manuf. Sci. Technol. **25**, 14–21 (2019)
3. Kuznetsov, Y., Prydalnyi, B., Redko, R.: Device for clamping rod-shaped material. Patent of Ukraine 95323 (2011)
4. Alquraan, T., Kuznetsov, Y., Tsvyd, T.: High-speed clamping mechanism of the CNC lathe with compensation of centrifugal forces. Procedia Eng. **150**, 689–695 (2016)

5. Fedorynenko, D., Sapon, S., Boyko, S.: Accuracy of spindle units with hydrostatic bearings. Acta Mech. Automatica **10**(2), 117–124 (2016)
6. Foremny, E., Schenck, C., Kuhfuß, B.: Dynamic behavior of an ultra precision spindle used in machining of optical components. Procedia CIRP **46**, 452–455 (2016)
7. Grossi, N., Scippa, A., Montevecchi, F., Campatelli, G.: A novel experimental-numerical approach to modeling machine tool dynamics for chatter stability prediction. J. Adv. Mech. Des. Syst. Manuf. **10**(2), 1–10 (2016)
8. Jia, Q., Li, B., Wei, Y., Chen, Y., Yuan, X.: Axiomatic design method for the hydrostatic spindle with multisource coupled information. Procedia CIRP **53**, 252–260 (2016)
9. Kono, D., Mizuno, S., Muraki, T., Nakaminam, M.: A machine tool motorized spindle with hybrid structure of steel and carbon fiber composite. CIRP Ann. **68**(1), 389–392 (2019)
10. Kuric, I., Cisar, M., Tlach, V., Zajacko, I., Gal, T., Wiecek, D.: Technical diagnostics at the department of dutomation and production systems. In: Burduk, A., Chlebus, E. (eds.) ISPEM 2018, Advances in Intelligent Systems and Computing, vol. 835, pp. 474–484. Springer, Cham (2019)
11. Zhang, L., Zha, J., Zou, C., Chen, X., Chen, Y.: A new method for field dynamic balancing of rigid motorized spindles based on real-time position data of CNC machine tools. Int. J. Adv. Manuf. Technol. **102**(5–8), 1181–1191 (2018). https://doi.org/10.1007/s00170-018-2953-2
12. Postel, M., Aslan, D., Wegener, K., Altintas, Y.: Monitoring of vibrations and cutting forces with spindle mounted vibration sensors. CIRP Ann. **68**(1), 413–416 (2019)
13. Rabréau, C., Ritou, M., Le Loch, S., Furet, B.: Investigation of the evolution of modal behavior of HSM Spindle at high speed. Procedia CIRP **58**, 405–410 (2017)
14. Ritou, M., Rabréau, C., Le Loch, S., Furet, B., Dumur, D.: Influence of spindle condition on the dynamic behavior. CIRP Ann. **67**(1), 419–422 (2018)
15. Wan, S., Hong, J., Du, F., Fang, B., Li, X.: Modelling and characteristic investigation of spindle-holder assembly under clamping and centrifugal forces. J. Mech. Sci. Technol. **33**(5), 2397–2405 (2019). https://doi.org/10.1007/s12206-019-0438-3
16. Thorenz, B., Westermann, H.-H., Kafara, M., Nützel, M., Steinhilper, R.: Evaluation of the influence of different clamping chuck types on energy consumption, tool wear and surface qualities in milling operations. Procedia Manuf. **21**, 575–582 (2018)
17. Yadav, M.H., Mohite, S.S.: Controlling deformations of thin-walled Al 6061–T6 components by adaptive clamping. Procedia Manuf. **20**, 509–516 (2018)
18. Zhang, S., Yu, J., To, S., Xiong, Z.: A theoretical and experimental study of spindle imbalance induced forced vibration and its effect on surface generation in diamond turning. Int. J. Mach. Tools Manuf. **133**, 61–71 (2018)